

# Erosion of a tungsten limiter under high heat flux in TEXTOR

G. Sergienko <sup>a,\*</sup>, B. Bazylev <sup>b</sup>, A. Huber <sup>a</sup>, A. Kreter <sup>a</sup>, A. Litnovsky <sup>a</sup>, M. Rubel <sup>c</sup>,  
V. Philipps <sup>a</sup>, A. Pospieszczyk <sup>a</sup>, Ph. Mertens <sup>a</sup>, U. Samm <sup>a</sup>, B. Schweer <sup>a</sup>,  
O. Schmitz <sup>a</sup>, M. Tokar <sup>a</sup>, The TEXTOR Team

<sup>a</sup> Institut für Plasmaphysik, Forschungszentrum Jülich GmbH, EURATOM Association, Trilateral Euregio Cluster, 52425 Jülich, Germany

<sup>b</sup> Institut für Hochleistungsimpuls und Mikrowellentechnik, Forschungszentrum Karlsruhe GmbH, 76021 Karlsruhe, Germany

<sup>c</sup> Alfvén Laboratory, Royal Institute of Technology, Association EURATOM-VR, 100 44 Stockholm, Sweden

## Abstract

Erosion characteristics of a tungsten plate heated up in TEXTOR by the plasma load have been investigated at temperatures extending to the melting point. No enhancement of atomic release exceeding physical sputtering and normal thermal sublimation for temperatures below 3700 K was observed. The liquid tungsten moved fast along the plate in the direction perpendicular to the magnetic field lines. The motion is caused by the Lorentz force due to the thermoelectron current emitted from the hot tungsten surface. The motion of liquid tungsten caused a material loss of 2.85 g during two discharges. The material redistribution due to the melt layer motion is compared with a MEMOS-1.5D simulation.

© 2007 Elsevier B.V. All rights reserved.

PACS: 52.40.Hf; 52.55.Fa; 32.20.Lg; 32.70.-n

Keywords: Tungsten; Limiter; Spectroscopy; Liquid metal; TEXTOR

## 1. Introduction

Tungsten (W) is foreseen as plasma-facing material for the upper divertor target in ITER. An experiment with a full W divertor is planned at JET to demonstrate the ability of W to replace carbon fibre compounds also at the high heat flux divertor areas of ITER. The main advantages are its low sputtering coefficient for expected particle impact and its low tritium retention capability. An open question

presently discussed is the possibility of an enhanced erosion of W at high temperatures, as reported for tungsten exposed to a high current argon plasma arc [1] and observed for beryllium [2]. Previous experiments carried out at TEXTOR [3] demonstrated that a tungsten test limiter could be heated up by the plasma to temperatures exceeding 3300 K when the limiter was inserted deep into the plasma (i.e., 2–3 cm inside the last closed flux surface (LCFS)). These experiments showed that oxygen can be released from the bulk at high temperatures. This complicates the analysis of the high temperature erosion due to the possible physical and chemical sputtering of oxidized metal. The

\* Corresponding author. Fax: +49 2461 612660.

E-mail address: [g.sergienko@fz-juelich.de](mailto:g.sergienko@fz-juelich.de) (G. Sergienko).

URL: [www.fz-juelich.de](http://www.fz-juelich.de) (G. Sergienko).

investigation of tungsten erosion under extreme conditions in the edge plasma of tokamaks is important to define the operational window for this material. Another question with W at the high heat flux areas is its ability to melt which may occur during high heat spikes resulting from transient events (e.g., VDEs, ELMs or disruptions). Possible melt layer loss or melt layer motion can strongly enhance the local erosion of the divertor tile and may also produce irregular surfaces which would be subject to hot spots in successive discharges. Investigations on the behaviour of melt layers in a strong magnetic field under high plasma heat flux are most important for an assessment of the applicability of W in these areas.

## 2. Measurements

A 2 mm thick polished solid tungsten plate with a size of  $75 \times 63 \text{ mm}^2$  was mounted on a graphite roof limiter with an angle of  $20^\circ$  with respect to the magnetic field lines. The thermal contact of the plate with the graphite substrate was lowered on purpose to ease the increase of the surface temperature. The surface temperature was measured by two single colour pyrometers (wavelength  $1.69 \mu\text{m}$  and  $1.58 \mu\text{m}$ ) at the position of maximum heat flux in the middle of the plate. The temperature distribution over the surface was measured by a video camera (20 ms time resolution) equipped with a long-pass filter with a cut-off at  $0.85 \mu\text{m}$ . The 2D distribution of the  $H_\beta$  ( $486.1 \text{ nm}$ ) line intensity and the motion of the liquid tungsten were measured with an intensified CCD video camera (20 ms time resolution) viewing tangentially to the limiter and equipped with an optical interference filter. Two thermocouples inserted into the graphite limiter through the holes at the ion and electron drift sides were used to measure the limiter base temperature and the total deposited energy. To evaluate the surface temperature from pyrometer signals, these were compared with the thermocouples in steady state prior to each discharge and corrected by the temperature dependent spectral emissivity of tungsten [4]. With this correction, an absolute accuracy of the surface temperature measurement of about 50 K was reached at the melting point.

The atomic W flux released from the plate was measured spectroscopically in the near UV region (280–308 nm) to reduce the influence of the thermal radiation continuum from the hot surface. For this purpose, a 0.5 m focal length spectrometer (ARC Spectra Pro500) equipped with an intensified CCD

camera (Proxitronic HL4) was used. The base limiter was preheated up to 629 K and inserted through a limiter lock into the plasma edge from the top of TEXTOR [5]. The vertical edges of the limiter were aligned parallel to the magnetic field lines and the W plate was placed on the ion drift side. The spectrometer entrance slit was perpendicular to the toroidal magnetic field and the viewing chords of the spectrometer were nearly tangential to surface of the tungsten plate. The main plasma parameters of TEXTOR during this experiment were:  $I_p = 355 \text{ kA}$ ,  $B_T = 2.25 \text{ T}$ ,  $\bar{n}_e = 4 \times 10^{13} \text{ cm}^{-3}$ ,  $a = 47.2 \text{ cm}$ ,  $n_e(a) = 4.4 \times 10^{12} \text{ cm}^{-3}$ ,  $T_e(a) = 32 \text{ eV}$ ,  $Z_{\text{eff}} \sim 1.4$ ,  $P_{\text{NBI}} = 1.2 \text{ MW}$  for 5 s,  $P_{\text{tot}} = 1.4 \text{ MW}$ , radiation level  $\gamma \approx 0.45$ .

The exposed tungsten was studied *ex-situ* by means of large scale profilometry (depth accuracy of  $1 \mu\text{m}$ , lateral accuracy of  $25 \mu\text{m}$ ), scanning electron microscopy (SEM) and energy dispersive X-ray analysis (EDX).

## 3. Experimental results and discussion

### 3.1. High temperature erosion

The position of the test limiter was changed radially shot-by-shot with steps of about 0.2 cm from one discharge to the next, resulting in the maximum surface temperature increasing from 870 K at  $r = 47.9 \text{ cm}$  inside the SOL to 3670 K for  $r = 46 \text{ cm}$  inside the LCFS. The heat flux density from the plasma evaluated calorimetrically from thermocouples increased exponentially with the limiter position and reached about  $5.5 \text{ MW/m}^2$  at the position  $r = 46 \text{ cm}$  where the erosion measurements have been made. A higher heat flux of  $8 \text{ MW/m}^2$  was obtained from the pyrometer measurements. This is due to the well known asymmetry of the heat flux between ion and electron side of the limiter [6]. In contrast to earlier measurements on solid W limiters [3], the spectroscopic measurements showed no measurable oxygen release from the hot tungsten plate up to 2300 K. This is due to a very low impurity content of the tungsten plate used in the present experiment. Many spectral W lines could be identified in the measured spectrum shown in Fig. 1. The W line intensities increased during discharge due to the strong rise of the W plate temperature. However, the line intensities do not always change proportionally to each other as shown in Fig. 2. The strongest lines WI (289.644 nm + 289.60 nm) and WI (294.440 nm + 294.699 nm) saturated at

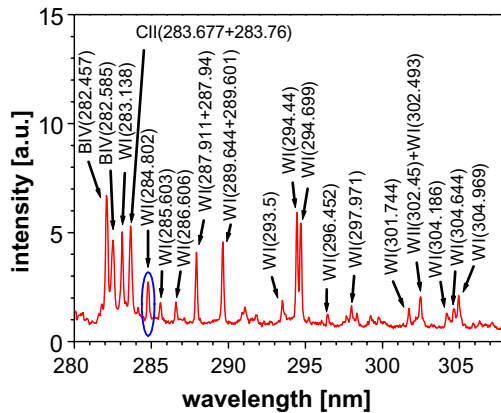


Fig. 1. Spectrum measured in front of the tungsten plate.

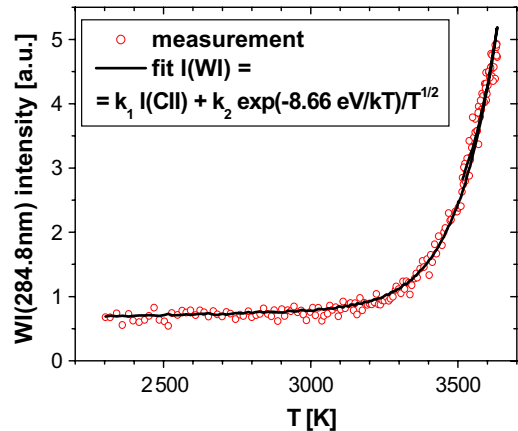


Fig. 3. Tungsten flux versus surface temperature.

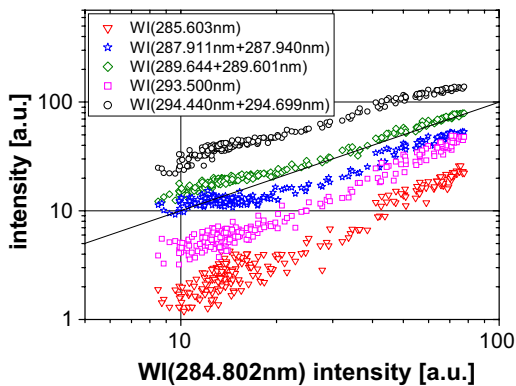


Fig. 2. Tungsten spectral line intensities versus the WI (284.802 nm) line intensity.

maximum intensities and the weakest line WI (285.603 nm) had a small signal-to-noise ratio. The WI (284.802 nm) spectral line marked in Fig. 1 was selected for the tungsten flux measurements because it had the best signal-to-noise ratio and was within the dynamic range of the ICCD camera of the spectrometer. It was found that the atomic tungsten flux from the plate was nearly constant up to a temperature of about 3200 K. With a further temperature rise, the flux grew exponentially by a factor of 7 at 3600 K (close to the melting point). The measured tungsten flux could be very well fitted by a sum of two fluxes, i.e., sputtering by carbon ions and regular evaporation of tungsten. The result of such fit is shown in Fig. 3.

The behaviour of the line intensities, which is stated above and shown in Fig. 2, indicates that sputtered and sublimated atoms have a different population of electronic states. This is because

sublimated atoms, released with a thermal energy below 0.3 eV, have about six times shorter penetration depth ( $\sim 0.3$  mm) in comparison with sputtered tungsten atoms having a mean kinetic energy of about 10 eV (as estimated by a formula from [7]) with a penetration depth into the plasma about 2 mm [8]. The electron energy distribution strongly changes near the surface due to the presence of thermo-electrons from the hot metal, thus affecting the excitation rates. The population of the ground state (especially the fine structure) of the sputtered atoms is different from those of evaporated atoms and this can also change the excitation. This could influence the accuracy of atomic tungsten flux measurement, which was made under the assumption that the line intensity is simply proportional to the neutral particle flux. Using the vapour pressure of tungsten from [9], the flux is estimated to be about  $4 \times 10^{17}$  atoms/cm<sup>2</sup> s at temperatures below 3000 K. This flux of sputtered tungsten atoms corresponds to about 1.4% of the plasma flux to the surface estimated from the heat flux density. The value is exclusively by carbon and oxygen induced sputtering and in a good agreement with previous measurements on tungsten limiters in TEXTOR [8,10].

### 3.2. Melt layer erosion

The melting of tungsten plate was intended in the experiment. It occurred only during two discharges with highest heat flux densities to the tungsten plate. The limiter was positioned at plasma radii of  $r = 46.0$  cm and 45.8 cm during these discharges when the toroidal magnetic field was ramped down from 2 T to 1.1 T over 2.17 s starting from the

beginning of the discharges. The peak heat flux density of about  $17 \text{ MW/m}^2$  was estimated in this case from calorimetric measurements. The tungsten melted poloidally along the plate edge at the region of the maximum heat flux at 1.93 s for  $r = 45.8 \text{ cm}$ . The liquid tungsten moved then perpendicularly to the magnetic field lines along the plate surface. The motion of liquid tungsten produced a deep furrow along the plate surface. A large blob of liquid metal reached the plate edge, from which two jets of molten material moved up (at 2 s) against gravity towards the scrape-off layer plasma along the edge of the graphite roof limiter. The width of the jets was about 3 mm. The velocity of the liquid jets estimated at the level of about 0.75 m/s was nearly constant within the first 2 cm of motion as observed by the tangentially viewing video camera. The jet propagated over a distance of about 5 cm. The discharges disrupted at 2.17 s when the  $q = 2$  magnetic surface reached the plasma edge. No material loss was observed during the disruption.

Profilometry studies have proven that the maximal thickness of the melt erosion was about 1 mm as shown in Fig. 4. Fig. 5 shows the material loss integrated over the toroidal direction. The total material loss during the existence of the liquid tungsten ( $\sim 1 \text{ s}$ ) was about of 2.85 g. Strong tungsten recrystallization (large grains and clearly visible grain boundaries) is found within about 3 cm from the plate edge positioned nearest to the plasma. The grain size has a maximum of 120–200  $\mu\text{m}$  in the melt zone due to the higher temperature and thicker melt layer at this position. No indications of blistering effects are found on the plate, neither in nor outside the melt-layer zone. Island-type inclusions of carbon containing particles (possible tungsten carbide) are detected in the eroded region. Small, dust-like spherical granules of tungsten are observed. The surface of the graphite limiter behind the hottest

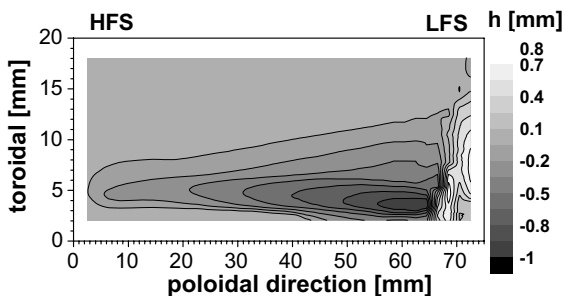


Fig. 4. Surface profile measured with 2 mm step in poloidal and 0.1 mm step in toroidal directions.

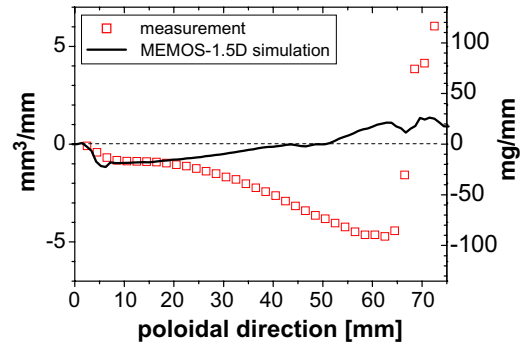


Fig. 5. Toroidally integrated tungsten redistribution.

part of the plate showed a clear visible tungsten coating. Intra-grain damages are observed on the edges of the erosion zone as shown in Fig. 6. Probably, the temperature in this region was close to the melting point and only parts of grains with reduced thermal contact due to cracking were preferentially molten and removed by the Lorentz force. The observed small, dust-like spherical granules can be a result of such erosion. This indicates a possible formation of tungsten dust when the metal melts in magnetic controlled fusion devices.

The motion of the liquid tungsten observed in TEXTOR can be interpreted by Lorentz forces induced by the thermoelectron emission from the hot surface. Numerical simulations of the melt motion damage of the tungsten plate have been performed in two steps. At the first step, the temperature distribution inside the tungsten plate including the molten layer was simulated without the melt layer motion with the 3-dimensional code PHEMOBRID-3D [11]. This enabled fitting of the heat load using the measured surface temperature as a fitting parameter. The calculated surface temperature

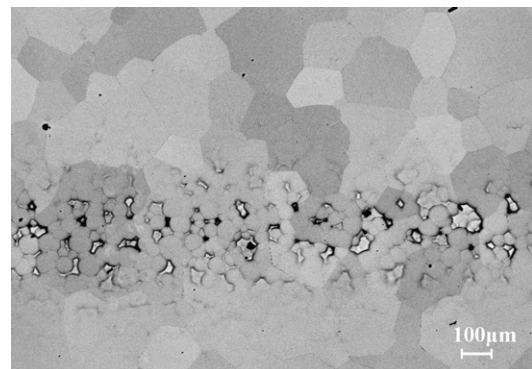


Fig. 6. SEM image of the edge of the melt erosion region.

agreed with the temperature measured by the pyrometer for the heat pulse duration of 1.66 s with a linear increase from 15 MW/m<sup>2</sup> to 24 MW/m<sup>2</sup>. The calculated maximum thickness of the melt layer reached 400 μm. At the second step, simulations of melt motion along the poloidal direction were performed by the quasi-one-dimensional fluid dynamics code MEMOS-1.5 code [12], which was modified to take into account the thermoelectron emission current according to [13]. The simulation showed fair agreement with experimental values of the melt layer erosion profile up to 20 mm from the HFS edge in poloidal direction as seen in Fig. 5 but disagrees for the larger distances. Whereas the measured melt erosion increases poloidally in the direction of melt layer motion, the simulation shows an accumulation of molten material in this direction. Such a discrepancy may appear because 3D effects were omitted in the simulation. The observed melt erosion inhomogeneity is probably due to the heat transfer to the solid tungsten substrate by the movement of the liquid tungsten. However, the plasma heat flux distribution may also change poloidally due to thermoelectron emission current, as observed in [14] and/or due to the influence of tungsten evaporation upon the heat flux transfer from the plasma to the surface. The results have shown that more experimental and modelling efforts are necessary. An extension of the code MEMOS to the 3D geometry is required to achieve better agreement aiming to take into account 3D and edge effects.

#### 4. Conclusions

Spectroscopic measurements of the atomic tungsten flux from a hot surface indicates that no enhancement of atomic tungsten release exceeding physical sputtering and normal thermal sublimation for temperatures below 3700 K occurs under the present experimental conditions.

Tungsten molten by plasma impact shows a rapid movement perpendicularly to magnetic field lines due to Lorentz forces caused by thermoelectron emission current. These forces are strong enough to move droplets of molten tungsten upwards against gravity. Numerical simulation by the MEMOS-1.5D code shows fair agreement with the measured melt layer

erosion but also deviations which calls for an extension of the code. Large tungsten re-crystallization and carbon inclusions were observed. The results show that melting can lead to a large material redistribution due to thermoelectron emission current without ejection of molten material. This may significantly influence the estimations of the lifetime of the ITER tungsten divertor and should be taken into account in the erosion assessment.

#### Acknowledgement

This work has been performed under the European Fusion Development Agreement in the frame of the European Task Force on Plasma–Wall Interaction.

#### References

- [1] E.P. Vaulin, N.E. Georgieva, T.P. Martynenko, L.V. Feoktistov, *Sov. J. Plasma Phys.* 7 (1981) 239.
- [2] R.P. Doerner, M.J. Baldwin, S.I. Krashennnikov, K. Schmid, J. Nucl. Mater. 337–339 (2005) 877.
- [3] M. Wada, T. Tanabe, V. Philipps, B. Unterberg, A. Pospieszczyk, B. Schweer, J. Rapp, Y. Ueda, K. Ohya, T. Ohgo, N. Noda, J. Nucl. Mater. 258–263 (1998) 853.
- [4] J.C. De Vos, *Physica* 20 (1954) 690.
- [5] B. Schweer, S. Brezinsek, H.G. Esser, A. Huber, Ph. Mertens, S. Musso, V. Philipps, A. Pospieszczyk, U. Samm, G. Sergienko, P. Wienhold, *Fusion Sci. Technol.* 47 (2005) 138.
- [6] M. Wada, T. Hirai, T. Ohgo, T. Tanabe, K. Ohya, V. Philipps, A. Huber, G. Sergienko, A. Pospieszczyk, N. Noda, J. Nucl. Mater. 313–316 (2003) 292.
- [7] G. Falcone, *Phys. Rev. B* 38 (1988) 6398.
- [8] V. Philipps, R. Neu, J. Rapp, U. Samm, M. Tokar, T. Tanabe, M. Rubel, *Plasma Phys. Control. Fus.* 42 (2000) B293.
- [9] T. Tanabe/High-Z Candidate Plasma Facing Materials Atomic and Plasma–Material Interaction Data for Fusion, vol. 5, IAEA, Vienna, 1994, p. 129.
- [10] V. Philipps, A. Pospieszczyk, A. Huber, A. Kirschner, J. Rapp, B. Schweer, P. Wienhold, G. van Oost, G. Sergienko, T. Tanabe, K. Ohya, M. Wada, T. Ohgo, M. Rubel, J. Nucl. Mater. 258–263 (1998) 858.
- [11] B.N. Bazylev, Y. Koza, I.S. Landman, J. Linke, S.E. Pestchanyi, H. Wuerz, *Phys. Scripta T111* (2004) 213.
- [12] B. Bazylev, H. Wuerz, *J. Nucl. Mater.* 307–311 (2002) 69.
- [13] S. Takamura, M.Y. Ye, T. Kuwabara, N. Ohno, *Phys. Plasmas* 5 (1998) 2151.
- [14] V. Philipps, U. Samm, M. Tokar, B. Unterberg, A. Pospieszczyk, B. Schweer, *Nucl. Fusion* 33 (1993) 953.